

1 **SARS-CoV-2 infection paralyzes cytotoxic and metabolic functions of immune cells**

2
3 Yogesh Singh^{1,2,6*#}, Christoph Trautwein^{3*}, Rolf Fendel^{4*}, Naomi Krickeberg⁴, Jana Held⁴,
4 Andrea Kreidenweiss⁴, Georgy Berezhnoy³, Rosi Bissinger⁵, Stephan Ossowski^{1,2}, Madhuri S.
5 Salker⁶, Nicolas Casadei^{1,2}, Olaf Riess^{1,2#} and the Deutsche COVID-19 OMICS Initiative
6 (DeCOI)

7
8 ¹Institute of Medical Genetics and Applied Genomics, University of Tübingen, Calwerstrasse
9 7, 72076, Tübingen, Germany

10
11 ²NGS Competence Center Tübingen (NCCT), University of Tübingen, Calwerstrasse 7, 72076
12 Tübingen, Germany

13
14 ³Werner Siemens Imaging Center, University of Tübingen, Röntgenweg 13, 72076, Tübingen,
15 Germany

16
17 ⁴Institute of Tropical Medicine, University Hospital of Tübingen, Tübingen, Wilhelmstrasse 27,
18 72076, Tübingen, Germany

19
20 ⁵Department of Internal Medicine, Division of Endocrinology, Diabetology and Nephrology,
21 University Hospital of Tübingen, Germany

22
23 ⁶Research Institute of Women's Health, University of Tübingen, Calwerstrasse 7/6, 72076,
24 Tübingen, Germany

25
26 *Equal contributions

27
28
29 # Correspondence

30 Dr Yogesh Singh or Prof Olaf Riess

31 Institute of Medical Genetics and Applied Genomics, Tübingen University

32 Calwerstraße 7, 72076, Tübingen, Germany

33 Phone: 0049 7071 29 72257/78264 Fax: 0049 7071 29 25355

34 Email: yogesh.singh@med.uni-tuebingen.de or olaf.riess@med.uni-tuebingen.de

35
36
37 **Key words:** COVID-19, CD8⁺ T cells, Granzyme B, Perforin, Metabolites

38
39
40 **Short title:** Defective immune-metabolic functions in COVID-19 patient

49 **Abstract:**

50

51 The SARS-CoV-2 virus is the causative agent of the global COVID-19 infectious disease
52 outbreak, which can lead to acute respiratory distress syndrome (ARDS). However, it is still
53 unclear how the virus interferes with immune cell and metabolic functions in the human body.
54 In this study, we investigated the immune response in 10 acute or convalescent COVID19
55 patients. We characterized the peripheral blood mononuclear cells (PBMCs) using flow
56 cytometry and found that CD8⁺ T cells were significantly subsided in moderate COVID-19 and
57 convalescent patients. Furthermore, characterization of CD8⁺ T cells suggested that patients
58 with a mild and moderate course of the COVID-19 disease and convalescent patients have
59 significantly diminished expression of both perforin and granzyme B in CD8⁺ T cells. Using ¹H-
60 NMR spectroscopy, we characterized the metabolic status of their autologous PBMCs. We
61 found that fructose, lactate and taurine levels were elevated in infected (mild and moderate)
62 patients compared with control and convalescent patients. Glucose, glutamate, formate and
63 acetate levels were attenuated in COVID-19 (mild and moderate) patients. Our findings reveal
64 patients who suffer from an over activation of the immune system, a change of composition in
65 infusion/intravenous fluids during infection with the aim to lower blood levels of glucose,
66 glutamate, acetate and formate could avoid a life-threatening cytokine storm. In summary, our
67 report suggests that SARS-CoV-2 infection leads to disrupted CD8⁺ T cytotoxic functions and
68 changes the overall metabolic functions of immune cells.

69

70

71

72

73

74

75

76

77

78

79

80

81

82

83

84

85

86

87

88

89

90

91

92

93

94

95

96

97 **Introduction:**

98 The first cases of severe acute respiratory coronavirus-2 (SARS-CoV-2) infection appeared in
99 December 2019, in Wuhan, China¹. This zoonotic virus has infected by now more than 26.1
100 million people (03.09.2020) and killed more than 0.86 million^{2,3} worldwide. The containment of
101 the pandemic is challenging and is still continuing with roughly 200,000 or more new infections
102 being reported daily since July 2020^{2,3}. There is an urgent need for a better understanding of
103 the immunopathology, as SARS-CoV-2 has become the leading cause of morbidity and
104 mortality in many countries.

105
106 Coronaviruses (CoV) are a large family of viruses that can cause illnesses such as the
107 common cold and seasonal influenza⁴. Pathologically, SARS-CoV-2 infects angiotensin-
108 converting enzyme 2 (ACE2)-expressing nasal epithelial cells in the upper respiratory tract
109 and type II alveolar epithelial cells in patients exhibiting pneumonitis^{1,5}. The most severe
110 disease courses led to death frequently but not exclusively in older patients with and without
111 risk conditions. The primary symptoms of SARS-CoV-2 infections are fatigue, fever, sore
112 throat, dry cough, loss of smell and taste within 5-21 days of incubation of the virus⁶⁻⁹. COVID-
113 19 symptoms are heterogeneous and range from asymptomatic to mild, moderate, and severe
114 pathological symptoms, presenting with or without pneumonia^{10,11}, however, most infected
115 people develop mild to moderate illness and recover without hospitalization^{12,13}. Primarily the
116 older COVID-19 patients can develop acute severe respiratory distress syndrome (ARDS) due
117 to a cytokine storm which is a life-threatening situation, requiring ventilation and intensive care
118 support¹⁴⁻¹⁸. High serum levels of IL-6, IL-8, IL-10, TNF- α cytokines and an immune hyper-
119 responsiveness referred to as a 'cytokine storm' is connected with poor clinical outcome^{19,20}.

120
121 Several break-through discoveries have extended our understanding how the virus takes
122 advantage of the host and modulates immunity^{12,17,21-25}. Recovered COVID-19 patients have
123 an increased number of antibody-secreting cells, activated CD4⁺ and CD8⁺ T cells, and
124 immunoglobulin M (IgM) and SARS-CoV-2 reactive IgG antibodies were detected in blood
125 before full symptomatic recovery²⁶⁻²⁸. Most severely affected COVID-19 patients had a lower
126 T cell but elevated B cell counts^{13,19,29,30}. Interestingly, patients with mild symptoms were
127 shown to have increased T and B cells compared with severely affected patients^{26,29-31}. There
128 could be several reasons for different disease outcomes including over-activated innate or
129 hyper-activated adaptive immune responses leading to cytokine storms and resulting in
130 severe injury to the lungs^{10,13,25,32}. Despite of several ongoing efforts, the immunological
131 mechanisms of the host-pathogen interaction are not well understood³³.

132
133 There is an intricate balance between the metabolic state of immune cells and generation of
134 immune response^{17,34-37}. CD8⁺ T cells require energy to proliferate and accomplish their
135 effective functions³⁸. Most propagating cells such as lymphocytes utilize the most abundant
136 energy substrates including, glucose, lipids, and amino acids³⁹. In response to SARS-CoV-2
137 and other virus infections, CD8⁺ T cells play a pivotal role in profound growth and proliferation
138 to generate their effective functional cells which can produce copious amounts of effector
139 molecules such as cytokines and cytotoxic granules^{30,38-40}. An activated immune system is
140 coupled with a change in metabolic reprogramming to produce enough energy needed during
141 (viral) infection^{38,39}. Proliferating T cells ferment glucose to lactate even in the presence of
142 oxygen to meet high energy demands^{34,37-39}. Furthermore, glucose and glutamine are involved
143 in the hexosamine biosynthetic pathway, which regulates the production of uridine

144 diphosphate N-acetyl glucosamine necessary for T cell clonal expansion and function⁴¹. The
145 synthesis of lactate intracellularly is crucial for T cells to have an increased glycolytic flux³⁸.

146

147 Peripheral blood mononuclear cells (PBMCs) can be analyzed to measure the health status
148 of an individual and can serve as a health biomarkers⁴². Therefore, the metabolic status of
149 lymphocytes could help to predict disease severity or to select the optimal therapeutic
150 intervention to boost the immune function during infection. Generally, most of the metabolism-
151 related functions in PBMCs during SARS-CoV-2 infections were inferred based on
152 transcriptomics analysis^{34,43} and no functional data (biochemical level) have been presented.
153 Thereof, understanding the kinetics of adaptive immune response as well as the metabolic
154 functions during SARS-CoV-2 infections will help to elucidate the host immune response to
155 SARS-CoV-2 infection. In this study, using flowcytometry and proton nuclear magnetic
156 resonance (¹H-NMR) spectroscopy, we characterized the PBMCs from SARS-CoV-2 infected
157 and convalescent patients for the their immunophenotypic and metabolic functions.

158

159 **Results:**

160

161 *Characteristics of study participants*

162

163 PBMCs were isolated and cryopreserved from blood samples obtained from COVID-19
164 patients suffering from mild ('Mild (outpatient)') or moderate/severe ('Moderate (inpatient)')
165 disease or were already recovered ('Convalescent') and from healthy controls ('HC').
166 Classification of disease severity for this analysis was based on the requirement of
167 hospitalization. Patients with mild COVID-19 were recruited within three days after
168 confirmation of infection by RT-qPCR. From moderate to severe COVID-19 patient blood
169 samples were collected one week after their admittance. The moderate patients were admitted
170 to the hospital requiring medical care, however, they did not need ventilation or O₂ supply.
171 Recovered patients were included based on a positive SARS-CoV-2 antibody testing. Study
172 participant characteristics are described in Table 2.

173

174 *Immunophenotyping of COVID-19 mild, moderate and convalescent COVID-19 patients*

175

176 To compare the number of lymphocytes and monocytes amongst the four study groups,
177 PBMCs were stained and analysed by flow cytometry. Both, lymphocytes (p=0.005) and
178 monocytes (p=0.04), were significantly decreased in moderate COVID-19 patients compared
179 with HC (Suppl. Fig. 1a, b). However, mild and convalescent patients also had a reduced, but
180 not significantly reduced, count of lymphocytes/monocytes compared to HC.

181

182 *Increased inflammatory monocytes and reduced NK cells in moderate COVID-19 patients*

183

184 Monocytes were further classified into classical, non-classical and intermediate based on
185 expression of CD14 and/or CD16 and we used the same gating strategies as described
186 earlier⁴⁴ (Suppl. Fig. 1c). We found that CD16⁺⁺CD14⁺ patrolling (non-classical) monocytes
187 were significantly increased (p=0.0008) in numbers in moderate patients compared to HC,
188 whereas this number is decreased again significantly compared with convalescent patients
189 (p=0.01) (Fig. 1a). The percentage of CD16⁺⁺CD14⁺ monocytes was also significantly
190 increased (p=0.006) in mild patients (outpatients) compared with moderate patients (Fig. 1a
191 Panel I). Interestingly, CD16⁺⁺CD14⁺⁺ pro-inflammatory monocytes (intermediate) were again

192 significantly increased in moderate ($p=0.003$) compared with HC as well as between mild and
193 HC ($p=0.02$) (Fig. 1a panel II). Furthermore, we observed a significantly reduced percentage
194 of CD14⁺⁺CD16⁻ phagocytic monocytes (classical) in moderate compared with mild
195 ($p=0.0009$), HC ($p<0.0001$) and convalescent ($p=0.0003$) patients (Fig. 1a Panel III). Finally,
196 we explored the lymphoid cells compartment for NK cells (CD56⁺CD3⁻CD19⁻). We found that
197 both mild ($p=0.0003$) and moderate ($p=0.0002$) patients were significantly different from
198 convalescent and HC ($p<0.0001$; HC vs mild or moderate) patients (Fig. 1b).

199

200 *Dynamics of B and T cells in mild, moderate and convalescent patients*

201

202 Both T and B cells are indispensable for the immune response against viral infections such as
203 SARS-CoV-2. Firstly, we compared the number of B cells amongst the study groups, which
204 give rise to virus-specific antibodies (see gating strategy in Suppl. Fig. 1c). The CD19⁺CD3⁻
205 cells (B cells) were significantly increased in mild ($p=0.008$; 1.7x times) and moderate
206 ($p=0.0008$; 1.9x times) patients compared with HC (Fig. 2a). Whilst, B cells were significantly
207 decreased in moderate compared to convalescent ($p=0.03$) patients (Fig. 2a). Comparing
208 CD3⁺CD19⁻ lymphocytes among the different patient groups we observed no significant
209 difference. However, there was an increased trend of CD3⁺ cells in the outpatients, inpatients
210 and convalescent groups compared with HC.

211

212 CD3⁺ cells were analysed for the CD4⁺ and CD8⁺ T cell compartment. There was a tendency
213 of increased CD4⁺ T cells for outpatients, inpatients and convalescent patients compared to
214 HC, but no significant difference was observed among any of the groups. CD8⁺ T cells were
215 significantly different between HC compared to moderate ($p=0.04$) or convalescent ($p=0.04$)
216 patients (Fig. 2b). Finally, we characterized CD4⁺Foxp3⁺CD45R⁻ regulatory T cells (Tregs),
217 however, no significant difference was observed among the different groups (Suppl. Fig. 2).

218

219 *Impaired activation and defective cytotoxic functions of CD8⁺ T cells*

220

221 We found that the percentage of CD8⁺ T cells was decreased in mild and convalescent
222 patients compared to HC. Thus, we explored the activation status of CD8⁺ T cells based on
223 HLA-DR expression. We found that CD8⁺ T cell activation status in all three groups of infected
224 patients were significantly different from HC (mild $p=0.01$, moderate $p=0.009$, and
225 convalescent $p=0.008$, Fig. 3a). We characterized the cytotoxic potential of CD8⁺ T cells based
226 on granzyme B and perforin levels and found that there was a tendency of decreased
227 granzyme B expression in mild, moderate and convalescent patients compared with HC (Fig.
228 3b), however it did not reach significance. Perforin was significantly decreased in convalescent
229 ($p=0.03$) patients compared with HC (Fig. 3b), although mild patients also had borderline
230 significantly reduced levels ($p=0.06$). Furthermore, we studied the expression of CD38, a
231 marker of cell activation, which was significantly upregulated in convalescent patients
232 compared with HC ($p=0.01$), mild ($p=0.03$) and moderate ($p=0.02$) patients (Fig. 4a). Similarly,
233 convalescent patients had significantly increased numbers of CD38⁺PD-1⁺ cytotoxic CD8⁺ T
234 cells compared with HC ($p=0.005$), moderate ($p=0.002$) and mild ($p=0.002$), which reflects the
235 exhaustion and non-responsiveness (anergy) of CD8⁺ T cells (Fig. 4b). Overall, our data
236 suggested that CD8⁺ T cells have reduced activation, diminished expression of cytotoxic
237 molecules such as perforin and granzyme B and severely exhausted phenotype.

238

239 *Dynamics of metabolites production in mild, moderate and convalescent patient*

240 PBMCs from all patient groups were subjected to ¹H-NMR spectroscopy analysis. We
 241 identified and quantified a total of 18 metabolites (Fig. 5a). Hereby, unsupervised PCA showed
 242 that spectral data from mild and moderate patients formed overlapping clusters clearly distinct
 243 from a cluster formed by HC and convalescent patients (Fig. 5b), indicating a strong difference
 244 in metabolite levels between infectious state compared to healthy or recovered state.
 245 Statistical analysis of the four different groups, revealed that 15 metabolites showed p-values
 246 < 0.05, with highest significance for metabolites from the energy metabolism (Fig. 5c, Suppl.
 247 Fig. 3 & Table 1). The data indicate a strong consumption of glucose, acetate, formate during
 248 infection, while with lactate levels are increased. Furthermore, we also found very high levels
 249 of fructose in PBMCs from mild patients, medium concentrations in moderate and, low levels
 250 in HC and convalescent patients (Fig. 5c). Furthermore, glutamate was almost abolished in
 251 mild and moderate patients, potentially as a consequence of enhanced production of α-
 252 ketoglutarate in the TCA cycle in PBMCs *via* glutamate dehydrogenase (Fig. 5c).

253
 254 To find an association between different metabolites, we applied the variable importance of
 255 projection (VIP) score. We found that formate and glucose had the highest score compared to
 256 another other metabolites (Fig. 6A). In order to determine if additional metabolites are
 257 positively associated with changes in glucose, lactate and fructose, we performed a pattern
 258 hunter analysis for all metabolites. We found that high glucose levels correlated with high
 259 formate, acetate and glutamate and low lactate and fructose (Fig. 6b), indicating enhanced
 260 glycolysis and TCA cycle in PBMCs. Similarly, fructose, that is entered *via* fructose-1-
 261 phosphate and dihydroxy acetone phosphate (DAP) into the glycolysis, is correlated positively
 262 with lactate and citrate and a decrease in acetate and formate, respectively (Fig. 6b).
 263 Interestingly, levels of the ROS scavenger taurine are only positively correlated with lactate
 264 and fructose, but not glucose (Fig. 6).

265

266 **Table 1: Summary of metabolites dysregulated in PBMCs**

267

No	Metabolites	HC	Mild	Moderate	Convalescent
1	Glucose	↑↑	↓↓	↓↓	↑↑
2	Formate	↑↑	↓↓↓	↓↓	↑↑
3	Acetate	↑	↓↓	↓	↑
4	Lactate	↓↓	↑↑	↑↑	↓↓
5	Fructose	↓	↑↑	↑	↓
6	Glutamate	↑	↓	↓	↑
7	Citrate	↓	↑↑	↑	↓
8	Taurine	↓↓	-	↑↑	↓
9	Creatine	↓	↑	-	-
10	Alanine	↓	-	↑↑	↓
11	Glycine	↑	↓	↓	-
12	Isoleucine	-	↓↓	↓	↑

268

269 To find an association between different metabolites, we applied the variable importance of
 270 projection (VIP) score. We found that formate and glucose had the highest score compared to
 271 other metabolites (Fig. 6A). In order to determine if additional metabolites are positively
 272 associated with changes in glucose, lactate and fructose, we performed a pattern hunter
 273 analysis for all metabolites. We found that high glucose levels correlated with high formate,

274 acetate and glutamate and low lactate and fructose (Fig. 6b), indicating enhanced glycolysis
275 and TCA cycle in PBMCs. Similarly, fructose, that is entered *via* fructose-1-phosphate and
276 dihydroxy acetone phosphate (DAP) into the glycolysis, is correlated positively with lactate
277 and citrate and a decrease in acetate and formate, respectively (Fig. 6b). Interestingly, levels
278 of the ROS scavenger taurine are only positively correlated with lactate and fructose, but not
279 glucose (Fig. 6).

280

281 **Discussion:**

282

283 SARS-CoV-2 infections are an intense and rapidly evolving area of research due to the
284 ongoing global pandemic^{19,25}. In this study, we used flow cytometry and ¹H-NMR to decipher
285 the cell proportions and functional state of immune cells (PBMCs) in mild, moderate and
286 convalescent COVID-19 patients compared to HC. Recent reports from COVID-19 patients
287 suggested that mild and severe patient had lymphopenia^{11,45-47}. Here, we found that mild
288 patients have reduced lymphocyte numbers whereas convalescent patients have recovered
289 the total lymphocyte counts. Similarly, monocytes were also reduced in mild patients, which is
290 in agreement with other recent studies^{29,48,49}. Importantly, our characterization of myeloid cell
291 compartment based on CD16 and CD14 markers suggested that non-classical and
292 intermediate monocytes were increased during an active mild or moderate SARS-CoV-2
293 infection, once infections are cleared the monocyte numbers return to normal. These results
294 are in accordance with some of the recent published studies^{48,50,51}, while another study
295 suggested the opposite⁵².

296

297 In our cohort, specifically CD56⁺NK cells were dramatically decreased during the course of
298 active SARS-CoV-2 viral infections (mild and moderate), while during recovery the numbers
299 were comparable to HC as report by others⁵³. Similarly another recent study suggested the
300 decrease in number of NK cell subsets in COVID-19 patients, with no change in CD56^{bright} or
301 CD56^{dim} cells⁵⁴. Thus, these data point to a crucial role of CD56⁺NK cells in eliminating SARS-
302 CoV-2 infections⁴⁷. CD19⁺ B lymphocytes were increased during the course of infection and
303 remain slightly higher than HC, thus reflecting the antibody response against the COVID-19
304 virus. Thus, this data implicated that these patients were able to generate the SARS-CoV-2
305 specific B cells.

306

307 A major difference was found in the T lymphocytes compartment. On the one hand, CD4⁺ T
308 cells were increased during infection, but not dramatically. On the other hand, CD8⁺ T cells
309 were significantly decreased in moderate and convalescent patients as reported earlier⁵³.
310 Thus, it appears that during viral infection non-virus specific CD8⁺ T cells are dead, while the
311 viral-specific surviving CD8⁺ T cells are clonally expanded but appeared to lost their effector
312 functions⁵⁵. To confirm this, we first measured the activation status of CD8⁺ T cells and found
313 that CD8⁺ T appeared to be less activated based on their HLA-DR activation marker²⁶. Further,
314 CD8⁺ T cells were examined for another activation marker CD38 which is involved in cell
315 adhesion, signal transduction and calcium signalling⁵⁶ and was found to be upregulated in
316 convalescent patients but not during active infection. These CD38⁺CD8⁺ T cells, were also
317 expressing higher levels of PD-1, which is an immune checkpoint and marker of
318 exhaustion^{24,30,49,57,58}. It guards against autoimmunity, promotes apoptosis of antigen-specific
319 T cells and promotes self-tolerance by suppressing T cell inflammatory activity. Thus, viral
320 infection leaves convalescent patients with exhausted phenotypes. We found that although
321 there was not a significant change in the numbers of Tregs in COVID-19 patients, there was

322 a trend towards elevated levels of Tregs in COVID-19 patients and rescued Tregs in
323 convalescent patients, in agreement with previous studies⁵⁷.

324

325 A key finding of our study was the surprising observation that granzyme B and perforin
326 secreting CD8⁺ T cells were significantly reduced in convalescent patients. The possible
327 implication of our finding is that convalescent patients, specifically including cancer patients
328 under treatment, could be susceptible to future opportunistic infections with other viruses
329 including different strains of SARS-CoV-2.

330

331 To date, the general metabolic physiology of PBMCs is not well defined in literature. However,
332 it is clear that PBMCs are dependent on circulating nutrients and hormones in the blood
333 system⁵⁹. The defective immune response in COVID-19 patients prompted us to investigate
334 the metabolic functions of these immune cells. Our metabolomics data indeed shows that
335 PBMCs from actively infected patients have a distinct metabolic profile from convalescent or
336 healthy individuals. The most notable difference we observed were for metabolites from the
337 glycolysis and oxidative phosphorylation (TCA cycle) pathway, which is in accordance with
338 recently published transcriptome data for PBMCs^{39,43}. Metabolites such as glucose, formate,
339 acetate and choline were also reduced in PBMCs in infected patients whereas, HC and
340 convalescent patients had a normal profile. Accordingly, the glycolytic pathway end products
341 such as lactate were higher in active mild and moderate COVID-19 patients compared with
342 HC and convalescent individuals. Therefore, our data suggests that PBMCs (which constitute
343 a major fraction of T lymphoid cells: 70- 80%) may have changed their metabolic functions,
344 particularly favouring the oxidative phosphorylation pathway over the glycolytic pathway, to
345 meet the high demands of energy needed to combat the ongoing viral infection.

346

347 A recent report suggested that elevated glucose levels enhance SARS-CoV-2 replication and
348 cytokine expression in monocytes and glycolysis sustains the viral-induced monocyte
349 response⁶⁰. Recently, it was emphasized that glucose consumption in PBMCs during COVID-
350 19 disease could be also a read-out of cytokine storms³⁴. Further, a higher abundance of
351 citrate in PBMCs suggested that perhaps T cells could use the oxidative phosphorylation
352 pathway for energy consumption to endure the infection, as recent transcriptomic data also
353 suggested that higher expression of genes related to oxidative phosphorylation both in
354 peripheral mononuclear leukocytes and bronchoalveolar lavage fluid (BALF) could play a
355 crucial role in increased mitochondrial activity during SARS-CoV-2 infection³⁴.

356

357 Another interesting finding of our study was the increase of fructose levels in PBMCs during
358 the course of infection. Previous findings suggested that fructose is involved in the
359 inflammatory pathways for the production of IL-1 β and IL-6 production⁶¹. Thus, it is possible
360 that the immune cells (most probably monocytes) could be triggered by higher fructose and
361 simultaneously induce inflammation and IFN- γ production by T cells⁶¹. These findings are
362 correlating with recent transcriptomic studies on the BALF from infected COVID-19 patients
363 and plasma of COVID-19 patients that also identified changes in fructose metabolism^{34,62}.

364

365 We finally observed a reduction of granzyme B and perforin in CD8⁺ T cells and detected the
366 antioxidant amino acid taurine, which could be involved in the cytotoxic functions of CD8⁺ T
367 cells. Both granzyme B and perforin are involved in ROS production and taurine serves as
368 ROS scavenger^{63,64}. Thus, decreased granzyme B and perforin could be implicated in reduced
369 ROS production for the impaired effectiveness of CD8⁺ T cells in convalescent or COVID-19

370 patients. This should be the case, as taurine levels that are generally increased during an
371 active infection in mild patients compared to healthy controls are not specifically decreasing
372 due to granzyme B and perforin lacking ROS activity in COVID-19 patients. However, this
373 finding needs further investigation to validate this hypothesis. In summary, the metabolomics
374 data generated in this study provides first and crucial insights into the complex metabolic
375 changes of PBMCs during SARS-CoV-2 infections, warranting further investigation.

376

377 **Conclusions:**

378 Using immunophenotyping and metabolomics approaches we detected significant changes in
379 PBMC samples of mildly and moderately affected COVID-19 as well as convalescent patients
380 compared to healthy controls. The significantly reduced amount of NK cells in both mild and
381 moderate patient groups corresponded with the clustering of PBMCs metabolite levels in the
382 principal component analysis distinct from the cluster formed by healthy and convalescent
383 individuals. The dramatic changed metabolic activity and pathways, such as glycolysis and
384 TCA cycle, might not only lead to a vulnerability of COVID-19 patients to subsequent
385 infections, but can also offer insights into how PBMCs could be manipulated towards a better
386 survival and personalized treatment of moderate and severe COVID-19 patients.

387

388 **Materials and Methods:**

389

390 **Ethics statement**

391 The study protocols were approved by the University of Tübingen, Germany Human Research
392 Ethics Committee (TÜCOV: 256/2020BO2 (convalescent study), COMIHY: (225/2020AMG1)
393 (outpatient study)-COMIHY, EUDRA-CT: 2020-001512-26, ClinicalTrials.gov
394 ID: NCT04340544, and COV-HCQ: (190//2020AMG1) (inpatient study)-COV-HCQ, EUDRA-
395 CT: 2020-001224-33, ClinicalTrials.gov ID: NCT04342221, 556/2018BO2) and all associated
396 procedures were carried out in accordance with approval guidelines. All participants provided
397 written informed consent in accordance with the Declaration of Helsinki.

398

399 **Study participants**

400

401 SARS-CoV-2 positive patients were used for this study and no other virus species were
402 analysed in this study (COMIHY and COV-HCQ). Blood was collected from COVID-19 patients
403 enrolled into two different prospective randomized, placebo-controlled, double blind clinical
404 trials evaluating safety and efficacy of hydroxychloroquine in COVID-19 outpatients
405 (COMIHY) and hospitalized patients (COV-HCQ). We analysed subsets of these study cohort
406 and used outpatient (n=3; COMIHY) which came to a specified outpatient ward at in the
407 Institute of Tropical Medicine with mild symptoms and blood was taken and usually defined as
408 D1 outpatients. Inpatients (n=3; COV-HCQ), blood was taken after 7-9 days after study
409 inclusion defined as D7. These patients had moderate symptoms needing hospital care,
410 however not being transferred to the intensive care unit in the hospital. Furthermore,
411 convalescent COVID-19 patients (n=4) were defined as positive for serum antibody reactive
412 to SARS-CoV-2 and blood was taken when they visited the Institute of Tropical Medicine for
413 testing of antibody levels. Amongst this cohort, 3 persons reported mild fever for 10-11 days
414 and 1 individual reported no fever but found positive for SARS-CoV-2 antibodies. Blood from
415 healthy controls (n=5) was obtained from the hospital blood bank.

416

417

418

419 **Table 2: Overview of study participants**
420

No	COVID-19 status	Blood sampling	COVID-19 severity	Sex	Age
1	Outpatient (mild)	Day1	mild	F	21
2	Outpatient (mild)	Day1	mild	M	59
3	Outpatient (mild)	Day1	mild	F	40
4	Inpatient (moderate)	Day7	Moderate	M	57
5	Inpatient (moderate)	Day7	Moderate	M	47
6	Inpatient (moderate)	Day7	Moderate	F	78
7	Convalescent (Sero +ve)	Convalescent	Recovered, healthy	F	50
8	Convalescent (Sero +ve)	Convalescent	Recovered, healthy	F	24
9	Convalescent (Sero +ve)	Convalescent	Recovered, healthy	M	50
10	Convalescent (Sero +ve)	Convalescent	Recovered, healthy	F	51
11	HC1	-	None	F	36
12	HC2	-	None	M	60
13	HC3	-	None	M	40
14	HC4	-	None	M	37
15	HC5	-	None	M	47

421
422 **Flow cytometry**

423
424 PBMCs were isolated by standard Ficoll method⁶⁵. A total of $1-2 \times 10^6$ PBMCs per participants
425 were used for three FACS panels (Table 2). In brief, cells were stained with surface markers
426 in DPBS (Sigma) with Super Bright stain Buffer (ThermoFisher) for 30 minutes at room
427 temperature (RT). To distinguish between live from dead, the cells were also incubated with
428 LIVE/DEAD Fixable Infra-Red Dead stain (ThermoFisher). After surface staining cells were
429 also stained for intracellular (IC) markers. Before IC staining, cells were fixed for 30-45 minutes
430 and permeabilized for 5 minutes followed by IC antibody incubation for additional 30 minutes
431 at RT. Cells were washed and resuspended in DPBS containing 2%FBS. Fixing of cells was
432 performed irrespective of whether panel was used for IC staining or not to prevent the possible
433 contamination during acquisition of the samples. For each sample 200,000 cells were acquired
434 using BD LSRFortessa (core facility) equipped with 4 lasers (violet, blue and yellow-green and
435 Red). Data were analysed using Flow Jo (Tree Star) and fluorescence minus one controls
436 (FMO) were used for setting up the arbitrary gates for the major cell markers.

437
438
439
440

441
442

Table 2: Antibodies and other reagents used for Flow cytometry

No.	Product Name	Clone	Fluorochrome	Product ID	Company
		NK cells and Monocytes (Panel 1)			
1	CD3	UCHT1	eFluor 450	48-0038-42	Thermofisher
2	CD4	SK3	SuperBright 600	63-0047-42	Thermofisher
3	CD8a	SK1	PerCP-eFluor 710	46-0087-42	Thermofisher
4	CD19	HIB19	eFluor 506	69-0199-42	Thermofisher
5	CD45-RA	HI100	PE-Cy7	25-0458-42	Thermofisher
6	HLA-DR	L243	Alexa Fluor647	A51010	Thermofisher
7	CD38	HIT2	PE-eFluor610	61-0389-42	Thermofisher
8	CD56	MEM188	PE	MA119638	Thermofisher
9	CD16	3G8	Super Bright702	67-0166-42	Thermofisher
10	CD14	61D3	Alexa Fluor700	56-0149-42	Thermofisher
11	Foxp3 (IC)	PCH101	FITC	11-4776-42	Thermofisher
		CD8 exhaustion, T helper follicular cells (Tfh) and antibody secreting cell (ASC) (Panel 2)			
1	CD3	UCHT1	eFluor 450	48-0038-42	Thermofisher
2	CD19	HIB19	eFluor 506	69-0199-42	Thermofisher
3	CD4	SK3	Super Bright 600	63-0047-42	Thermofisher
4	CD8a	SK1	PerCP-eFluor 710	46-0087-42	Thermofisher
5	CD38	HIT2	PE-eFluor 610	61-0389-42	Thermofisher
6	CD27	O323	Alexa Fluor700	56-0279-42	Thermofisher
7	CXCR5 (CD185)	MU5UBE E	FITC	11-9185-42	Thermofisher
8	ICOS (CD278)	C398.4A	PE	12-9949-81	Thermofisher
9	PD-1 (CD279)	eBioJ105 (J105)	PE-Cy7	25-2799-42	Thermofisher
10	HLA-DR	L243	Alexa Fluor647	A51010	Thermofisher
		Cytotoxic potential			
1	CD4	SK3	SuperBright600	63-0047-42	Thermofisher
2	CD8	SK1	PerCP-eFluor710	46-0087-42	Thermofisher
3	CD19	HIB19	eFluor 506	69-0199-42	Thermofisher
4	CD38	HIT2	PE-eFluor 610	61-0389-42	Thermofisher
5	HLA-DR	L243	Alexa Fluor 647	A51010	Thermofisher

6	GZMA (IC)	CB9	Alexa Fluor 488		Thermofisher
7	GZMB (IC)	GB11	PE	MA523639	Thermofisher
8	Perforin (IC)	dG9	PE-Cy7	12-9177-42	Thermofisher
		Other Flow reagents			
1	Ultracompensation bead			01-2222-42	Thermofisher
2	FOXP3/TRN FACTOR STAIN BUFFER SET			00-5523-00	Thermofisher
3	FLOW STAIN BUFFER SOLN			00-4222-57	Thermofisher
4	SB COMPLETE STAINING BUFFER			SB-4401-42	Thermofisher
5	DPBS			D8537	Sigma
6	Pancoll human			P04-601000	Pan Biotech

443

444 **¹H-NMR metabolomics**

445

446 To obtain PBMCs metabolites, PBMCs were suspended in an optimized solvent extraction
 447 mixture of 9:1 (methanol:chloroform) as described elsewhere in detail⁶⁶ and extracted with a
 448 focused ultrasound system (Covaris E220, Woburn, USA). The extraction solutions were
 449 evaporated to dryness for 4 hours in a vacuum concentrator and afterwards pellets
 450 resuspended with 45 μ L in a 1 mM TSP containing deuterated phosphate buffer. After
 451 centrifugation at 20,000 x g for 10 min to remove residual macromolecules, 40 μ L of the clear
 452 supernatant were transferred to 1.7 mm NMR tubes. Spectra were recorded on an
 453 ultrashielded 600 MHz spectrometer (Bruker AVANCE III HD, Karlsruhe, Germany) with a
 454 triple resonance 1.7 mm room temperature probe. Spectra used for analysis were acquired
 455 with a 2h 55min lasting CPMG pulse program. Metabolite annotation and quantification was
 456 done with ChenomX NMR Suite 8.3.

457

458 **Statistical analysis**

459

460 Bar diagrams were prepared using GraphPad Prism 6.0. FACS data were analysed using one-
 461 way ANOVA for multiple group comparisons (mild, moderate, convalescent and HC) in
 462 GraphPad Prism software. No matching or pairing was used. Assumed Gaussian distribution
 463 with equal standard deviations (SDs) for experimental design. Mean of each group was
 464 compared with the mean of every other group and Tukey's post-hoc tests for multiple
 465 comparisons. P value considered significant less than 0.05. Metabolites data were analysed
 466 with MetaboAnalyst 4.0 software.

467

468

469

470

471

472

473

474 **Figure legends:**

475

476 **Fig. 1:** Comparison of monocytes and NK cell percentage amongst study groups.

477

478 A. The stained PBMCs were gated on the monocyte population and CD3+CD19+ cells
479 were excluded. Cell populations are displayed for CD16 and CD14 expression (upper
480 FACS panel). One exemplary dot plot is shown per study group. The bar diagrams
481 (lower panel) show the non-classical (CD16⁺⁺CD14⁺), intermediate (CD16⁺⁺CD14⁺⁺)
482 and classical (CD16⁻CD14⁺⁺) monocytes. *P value <0.05, **P value <0.01 and ***P
483 value <0.001.

484 B. The stained PBMCs were gated on lymphocyte population and further excluded the
485 CD3+CD19+ cells and examined for the CD56 and CD16 expression in HC, mild,
486 moderate and convalescent (upper FACS panel). One exemplary dot plot is shown per
487 study group. The bar diagram shows the CD56⁺CD3⁻CD19⁻ NK cells. **P value <0.01
488 and ****P value <0.0001.

489

490 **Fig. 2:** Increased B cells in mild and moderate patients and reduced CD8⁺ cytotoxic T cells in
491 mild and convalescent patients

492

493 A. The stained PBMCs were gated on lymphocyte population and examined for the CD19
494 and CD3 expression in HC, mild, moderate and convalescent (upper FACS panel).
495 One exemplary dot plot is shown per study group. The bar diagram shows CD3⁻CD19⁺
496 B cells. *P value <0.05, **P value <0.01 and ***P value <0.001.

497 B. The CD19⁻CD3⁺ lymphocytes were examined for CD4⁺ and CD8⁺ T marker expression.
498 One exemplary dot plot is shown per study group. There was statistically significant
499 difference among HC, mild, moderate and convalescent (upper FACS panel).
500 However, CD8⁺ T cells were significantly reduced in outpatient and convalescent
501 patients. *P value <0.05.

502

503 **Fig. 3:** Decreased activation and cytotoxic functional protein expression of CD8⁺ T cells in
504 convalescent patients

505

506 A. CD8⁺ T cells were examined for the expression of activation marker HLA-DR (upper
507 FACS panel). One exemplary dot plot is shown per study group. The bar diagram
508 (lower panel) shows that HLA-DR was significantly lower on CD8⁺ T cells in mild,
509 moderate and convalescent COVID-19+ patients compared with HC.

510 B. CD8⁺ T cells were examined for the expression of their cytotoxic potential using
511 granzyme B and perforin expression using IC staining (upper FACS panel). One
512 exemplary dot plot is shown per study group. There was statistically significant
513 difference among HC, mild, moderate and convalescent (upper FACS panel) for
514 granzyme B. The bar diagram (lower panel) shows that perforin expression was
515 significantly lower on CD8⁺ T cells in convalescent COVID-19+ patients compared with
516 HC, though mild and moderate represent lower expression of perforin, but it did not to
517 a significant level. *P value <0.05.

518

519 **Fig. 4:** Increased exhausted CD8⁺ T cells in convalescent patients

520

- 521 A. Expression of activation marker CD38 on CD8⁺ T cells (upper FACS panel). One
522 exemplary dot plot is shown per study group. The bar diagram (lower panel) shows
523 that CD38 expression was significantly higher on CD8⁺ T cells in convalescent COVID-
524 19+ patients compared with HC. *P value <0.05.
525
- 526 B. Expression of activation marker CD38 and PD-1 on CD8⁺ T cells (upper FACS panel).
527 One exemplary dot plot is shown per study group. The bar diagram (lower panel)
528 shows that PD-1⁺CD38⁺ expression on was significantly higher on CD8⁺ T cells in
529 convalescent COVID-19+ patients compared with HC. *P value <0.05, **P value <0.01.
530

531 **Fig. 5:** ¹H-NMR spectroscopy of PBMC extracts

- 532 A. Heatmap of featured metabolites' concentrations plotted with SARS-CoV-2
533 progression group clustering.
534 B. Principle component analysis (PCA) was performed to identify the clustering of two
535 different groups. HC and convalescent COVID-19 patient samples cluster together
536 while SARS-Co-2 infected mild and moderate patients cluster in a separate cluster with
537 PC1: 90.7% and PC2: 2.6%.
538 C. Box plots for differentially abundantly present metabolites in different group including
539 HC, mild, moderate, and convalescent COVID-19 patient. *P value <0.05, **P value
540 <0.01 and ***P value <0.001.
541

542 **Fig. 6:** Pattern hunter plots provide an insight of close correlations with other metabolites
543 during COVID-19 infection.

- 544 A. Variable Importance in Projection (VIP) scores for all metabolites in the four studied
545 groups.
546 B. Pattern hunter plot for glucose.
547 C. Pattern hunter plot for lactate and fructose.
548

549 **Suppl. Fig. 1:** Total % counts of monocytes and lymphocytes from PBMCs of COVID-19
550 patients.

- 551 A. Fixed PBMCs samples were acquired on flow cytometry on 2-3 different days for the
552 entire experiments. Total 200,000 cells were acquired by flow cytometry and gating
553 was performed based on FSC and SSC parameters for lymphocytes, monocytes and
554 dead cells as described earlier⁶⁷⁻⁶⁹.
555 B. The bar graphs represent the % of lymphocytes and monocytes.
556 C. Gating strategy for T lymphocytes (CD3, CD4 and CD8) monocytes (CD14 and
557 CD16)⁴⁴, NK cells (CD56) using FMO controls.
558

559 **Suppl. Fig. 2:** Kinetics of regulatory T cells is not affected significantly in mild, moderate and
560 convalescent patients.

- 561
562 Foxp3⁺ expression on CD19⁻CD3⁺CD4⁺CD45RA⁻ T cells to identify the regulatory T cells in
563 HC, outpatient, outpatient and convalescent (upper FACS panel). There was statistically
564 significant difference among HC, mild, moderate and convalescent (upper FACS panel).
565

566 **Suppl. Fig. 3:** Metabolite analysis in COVID-19 patients

- 567 A. Analysis of Variance (ANOVA) for multi-group comparisons
568 B. Partial Least Squares Discriminant Analysis (PLSDA) scores plot

569 C. Hierarchical clustering of metabolites (distance measured with Pearson r correlation
570 coefficient)

571 D. Boxplots for branched chain amino acids valine and leucine

572

573 **Authors contributions:**

574

575 YS: Overall study design and project coordination, flow cytometry experiments, data analysis
576 and interpretation and initial metabolic sample preparation, funding generation, and writing the
577 manuscript.

578 CT: Metabolites sample preparation, Processing of the sample on ¹H-NMR, data analysis,
579 data interpretation and writing

580 MO: Metabolites sample preparation, Processing of the sample on ¹H-NMR

581 RF, NK: Provided patient materials, Isolation of PBMCs, Performed the experiments for
582 flowcytometry in BSL-2 facility, flow data interpretations.

583 JH, AK: Coordination of the clinical trials, revision of the manuscript.

584 RB: Isolation of PBMCs from HC and sample preparation for flow cytometry.

585 SO, MS, NC, OR: Study design, providing research tools, funding generation, data
586 interpretation and writing and amending the manuscript.

587

588 All the authors have seen the manuscript, substantially contributed and agreed to be co-
589 author.

590

591 **Acknowledgements:**

592

593 We thank you all the patients who participated in this study and FACS core facility (Klinikum-
594 Berg) for accessing the Flow cytometry for the experiments. We acknowledge support by
595 Deutsche Forschungsgemeinschaft (DFG) and Open Access Publishing Fund of University of
596 Tübingen.

597

598 **Funding:**

599

600 RB is supported by Deutsche Forschungsgemeinschaft (DFG Project no. 426724658). EKFS
601 (MS), DFG (OR), Ferring Pharmaceutical (YS and MS). Funders have no role in the study
602 design and data analysis. The German Federal Ministry of Education and Research (BMBF)
603 (BMBF-01KI2052) and the German Federal Ministry of Health (BMG) (BMG-ZMV11-
604 1520COR801).

605

606 **Competing interests:**

607

608 Authors declare no financial competing interests.

609

610 **Consortia**

611 The members of the Deutsche COVID-19 Omics Initiative (DeCOI) are Angel Angelov, Robert
612 Bals, Alexander Bartholomäus, Anke Becker, Daniela Bezdán, Ezio Bonifacio, Peer Bork,
613 Nicolas Casadei, Thomas Clavel, Maria Colome-Tatche, Andreas Diefenbach, Alexander
614 Diltthey, Nicole Fischer, Konrad Förstner, Julia-Stefanie Frick, Julien Gagneur, Alexander
615 Goemann, Torsten Hain, Michael Hummel, Stefan Janssen, Jörn Kalinowski, René Kallies,
616 Birte Kehr, Andreas Keller, Sarah Kim-Hellmuth, Christoph Klein, Oliver Kohlbacher, Jan O.

617 Korbel, Ingo Kurth, Markus Landthaler, Yang Li, Kerstin Ludwig, Oliwia Makarewicz, Manja
618 Marz, Alice McHardy, Christian Mertes, Markus Nöthen, Peter Nürnberg, Uwe Ohler, Stephan
619 Ossowski, Jörg Overmann, Silke Peter, Klaus Pfeffer, Anna R. Poetsch, Alfred Pühler,
620 Nikolaus Rajewsky, Markus Ralser, Olaf Rieß, Stephan Ripke, Ulisses Nunes da Rocha, Philip
621 Rosenstiel, Antoine-Emmanuel Saliba, Leif Erik Sander, Birgit Sawitzki, Philipp Schiffer, Eva-
622 Christina Schulte, Joachim L. Schultze, Alexander Sczyrba, Yogesh Singh, Oliver Stegle, Jens
623 Stoye, Fabian Theis, Janne Vehreschild, Jörg Vogel, Max von Kleist, Andreas Walker, Jörn
624 Walter, Dagmar Wieczorek, and John Ziebuhr.

625

626 **References:**

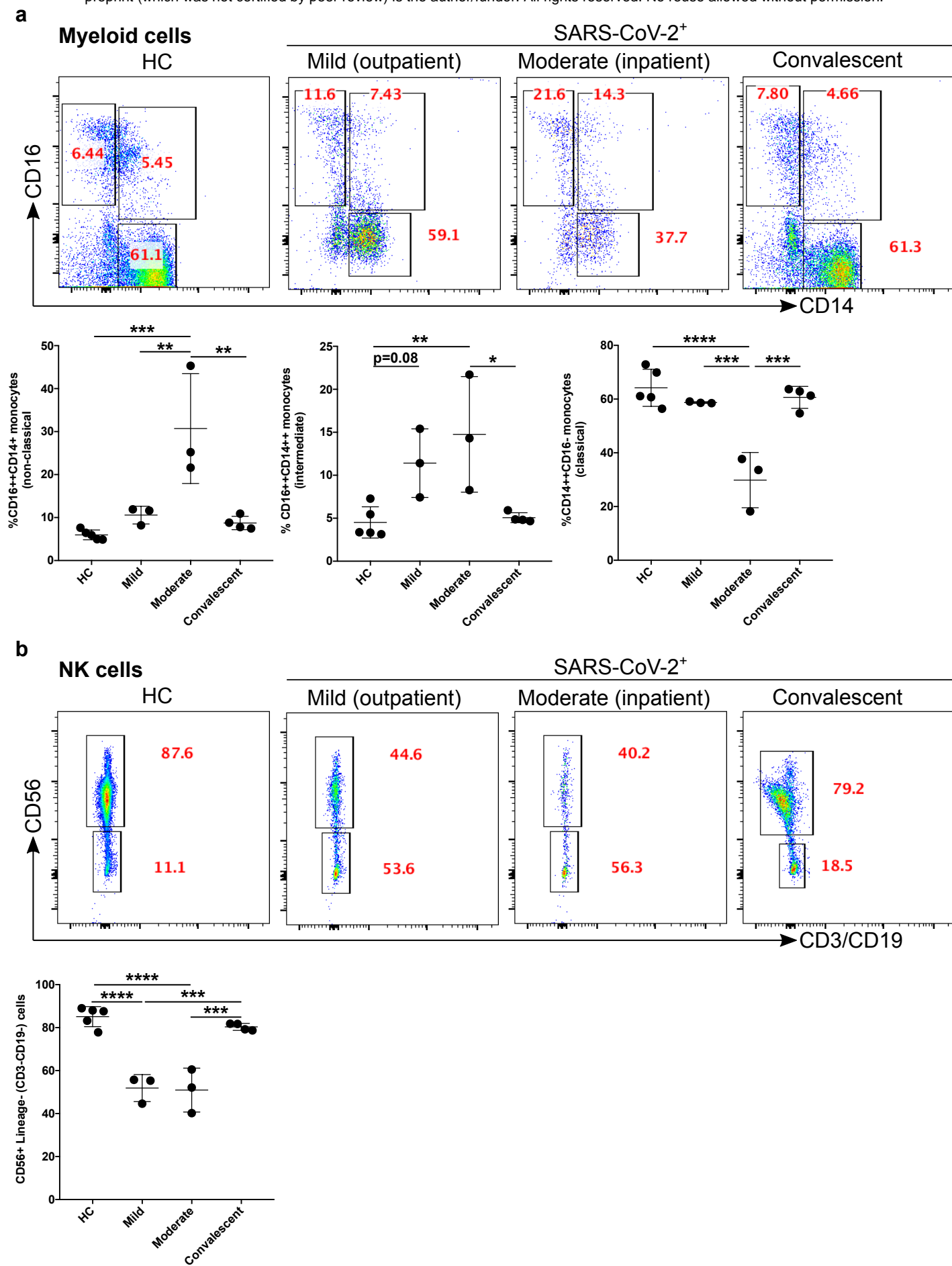
627

- 628 1 Zhu, N. et al. A Novel Coronavirus from Patients with Pneumonia in China, 2019. *N*
629 *Engl J Med* 382, 727-733, doi:10.1056/NEJMoa2001017 (2020).
- 630 2 Dashboard, J. C.-L. <https://coronavirus.jhu.edu/map.html>. (2020).
- 631 3 Dashboard, W. L. <https://covid19.who.int>. (2020).
- 632 4 Chang, L., Yan, Y. & Wang, L. Coronavirus Disease 2019: Coronaviruses and Blood
633 Safety. *Transfus Med Rev*, doi:10.1016/j.tmr.2020.02.003 (2020).
- 634 5 Lehner, N. J. M. P. J. How does SARS-CoV-2 cause COVID-19? *Science*, 510-511
635 (2020).
- 636 6 Liu, J. et al. Community Transmission of Severe Acute Respiratory Syndrome
637 Coronavirus 2, Shenzhen, China, 2020. *Emerg Infect Dis* 26,
638 doi:10.3201/eid2606.200239 (2020).
- 639 7 Singhal, T. A Review of Coronavirus Disease-2019 (COVID-19). *Indian J Pediatr* 87,
640 281-286, doi:10.1007/s12098-020-03263-6 (2020).
- 641 8 WHO. <WHO-2019-nCoV-Sci_Brief-Transmission_modes-2020.3-eng.pdf>. WHO
642 Report (2020).
- 643 9 Rothe, C. et al. Transmission of 2019-nCoV Infection from an Asymptomatic Contact
644 in Germany. *N Engl J Med* 382, 970-971, doi:10.1056/NEJMc2001468 (2020).
- 645 10 Xu, Z. et al. Pathological findings of COVID-19 associated with acute respiratory
646 distress syndrome. *The Lancet Respiratory Medicine* 8, 420-422, doi:10.1016/s2213-
647 2600(20)30076-x (2020).
- 648 11 Wei Huang, J. B., Michelle McNamara, Suraj Saksena, Marsha Hartman, Tariq Arshad,
649 Scott J. Bornheimer and Maurice O'Gorman. Lymphocyte Subset Counts in COVID-19
650 Patients: A Meta-Analysis. doi:10.1002/cyto.24172 (2020).
- 651 12 Chen, G. et al. Clinical and immunological features of severe and moderate
652 coronavirus disease 2019. *J Clin Invest* 130, 2620-2629, doi:10.1172/JCI137244
653 (2020).
- 654 13 Shi, Y. et al. COVID-19 infection: the perspectives on immune responses. *Cell Death*
655 *Differ*, doi:10.1038/s41418-020-0530-3 (2020).
- 656 14 NcA OANA dOcEA, A. T., DANA ALBULEScU, OANA CRISTEA, & OVIDIU ZLATIAN,
657 M. V., STERGHIOS A. MOSCHOS, dIMITRIS TSOUKALAS, MARINA GOUMENOU,
658 NIKOLAOS dRAKOULIS, JOSEF M. dUMANOV, VIcTOR A. TUTELYAN, GENNAdII
659 G. ONISCHENKO, MIcHAEL ASCHNER, dEMETRIOS A. SPANdIdOS and dANIELA
660 cALINA. A new threat from an old enemy: Re-emergence of coronavirus (Review).
661 *INTERNATIONAL JOURNAL OF MOLEcULAR MEdIcINE* 45, 1631-1643 (2020).
- 662 15 Ong, E. Z. et al. A Dynamic Immune Response Shapes COVID-19 Progression. *Cell*
663 *Host Microbe* 27, 879-882 e872, doi:10.1016/j.chom.2020.03.021 (2020).
- 664 16 Picchianti Diamanti, A., Rosado, M. M., Pioli, C., Sesti, G. & Lagana, B. Cytokine
665 Release Syndrome in COVID-19 Patients, A New Scenario for an Old Concern: The
666 Fragile Balance between Infections and Autoimmunity. *Int J Mol Sci* 21,
667 doi:10.3390/ijms21093330 (2020).
- 668 17 Vabret, N. et al. Immunology of COVID-19: Current State of the Science. *Immunity* 52,
669 910-941, doi:10.1016/j.immuni.2020.05.002 (2020).

- 670 18 Velavan, T. P. & Meyer, C. G. Mild versus severe COVID-19: Laboratory markers. *Int*
671 *J Infect Dis* 95, 304-307, doi:10.1016/j.ijid.2020.04.061 (2020).
- 672 19 Daniela Weiskopf¹, K. S. S., Matthijs P. Raadsen, Alba Grifoni, Nisreen M.A. Okba,
673 Henrik Endeman, Johannes P.C. van den Akker, Richard Molenkamp, Marion P.G.
674 Koopmans, Eric C.M. van Gorp, Bart L. Haagmans, Rik L. de Swart, Alessandro Sette,
675 Rory D. de Vries. Phenotype and kinetics of SARS-CoV-2-specific T cells in COVID-
676 19 patients with acute respiratory distress syndrome. *Science Immunology*,
677 doi:10.1126/sciimmunol.abd2071 (2020). (2020).
- 678 20 Del Valle, D. M. et al. An inflammatory cytokine signature predicts COVID-19 severity
679 and survival. *Nature Medicine*, doi:10.1038/s41591-020-1051-9 (2020).
- 680 21 Wu, H. et al. Clinical and Immune Features of Hospitalized Pediatric Patients With
681 Coronavirus Disease 2019 (COVID-19) in Wuhan, China. *JAMA Netw Open* 3,
682 e2010895, doi:10.1001/jamanetworkopen.2020.10895 (2020).
- 683 22 Du, S. Q. & Yuan, W. Mathematical modeling of interaction between innate and
684 adaptive immune responses in COVID-19 and implications for viral pathogenesis. *J*
685 *Med Virol*, doi:10.1002/jmv.25866 (2020).
- 686 23 Giamarellos-Bourboulis, E. J. et al. Complex Immune Dysregulation in COVID-19
687 Patients with Severe Respiratory Failure. *Cell Host Microbe* 27, 992-1000 e1003,
688 doi:10.1016/j.chom.2020.04.009 (2020).
- 689 24 Braciale, T. J. & Hahn, Y. S. Immunity to viruses. *Immunol Rev* 255, 5-12,
690 doi:10.1111/imr.12109 (2013).
- 691 25 McKechnie, J. L. & Blish, C. A. The Innate Immune System: Fighting on the Front Lines
692 or Fanning the Flames of COVID-19? *Cell Host Microbe* 27, 863-869,
693 doi:10.1016/j.chom.2020.05.009 (2020).
- 694 26 Thevarajan, I. et al. Breadth of concomitant immune responses prior to patient
695 recovery: a case report of non-severe COVID-19. *Nature Medicine*,
696 doi:10.1038/s41591-020-0819-2 (2020).
- 697 27 Assis, R. R. d. et al. Analysis of SARS-CoV-2 Antibodies in COVID-19 Convalescent
698 Plasma using a Coronavirus Antigen Microarray
699 bioRxiv preprint doi: <https://doi.org/10.1101/2020.04.15.043364>,
700 doi:10.1101/2020.04.15.043364 (2020).
- 701 28 Cao, Y. et al. Potent Neutralizing Antibodies against SARS-CoV-2 Identified by High-
702 Throughput Single-Cell Sequencing of Convalescent Patients' B Cells. *Cell* 182, 73-84
703 e16, doi:10.1016/j.cell.2020.05.025 (2020).
- 704 29 Qin, C. et al. Dysregulation of immune response in patients with COVID-19 in Wuhan,
705 China. *Clin Infect Dis*, doi:10.1093/cid/ciaa248 (2020).
- 706 30 Song, J. W. et al. Immunological and inflammatory profiles in mild and severe cases
707 of COVID-19. *Nat Commun* 11, 3410, doi:10.1038/s41467-020-17240-2 (2020).
- 708 31 Channappanavar, R., Fett, C., Zhao, J., Meyerholz, D. K. & Perlman, S. Virus-specific
709 memory CD8 T cells provide substantial protection from lethal severe acute respiratory
710 syndrome coronavirus infection. *J Virol* 88, 11034-11044, doi:10.1128/JVI.01505-14
711 (2014).
- 712 32 Janice Oh, H. L., Ken-En Gan, S., Bertoletti, A. & Tan, Y. J. Understanding the T cell
713 immune response in SARS coronavirus infection. *Emerg Microbes Infect* 1, e23,
714 doi:10.1038/emi.2012.26 (2012).
- 715 33 Bost, P. et al. Host-Viral Infection Maps Reveal Signatures of Severe COVID-19
716 Patients. *Cell*, doi:10.1016/j.cell.2020.05.006 (2020).
- 717 34 Gardinassi, L. G., Souza, C. O. S., Sales-Campos, H. & Fonseca, S. G. Immune and
718 Metabolic Signatures of COVID-19 Revealed by Transcriptomics Data Reuse.
719 *Frontiers in Immunology* 11, doi:10.3389/fimmu.2020.01636 (2020).
- 720 35 Ayres, J. S. Immunometabolism of infections. *Nat Rev Immunol* 20, 79-80,
721 doi:10.1038/s41577-019-0266-9 (2020).
- 722 36 Thaker, S. K., Ch'ng, J. & Christofk, H. R. Viral hijacking of cellular metabolism. *BMC*
723 *Biol* 17, 59, doi:10.1186/s12915-019-0678-9 (2019).

- 724 37 Moreno-Altamirano, M. M. B., Kolstoe, S. E. & Sanchez-Garcia, F. J. Virus Control of
725 Cell Metabolism for Replication and Evasion of Host Immune Responses. *Front Cell*
726 *Infect Microbiol* 9, 95, doi:10.3389/fcimb.2019.00095 (2019).
- 727 38 Gupta, S. S., Wang, J. & Chen, M. Metabolic Reprogramming in CD8+ T Cells During
728 Acute Viral Infections. *Frontiers in Immunology* 11, doi:10.3389/fimmu.2020.01013
729 (2020).
- 730 39 Shehata, H. M. et al. Sugar or Fat?-Metabolic Requirements for Immunity to Viral
731 Infections. *Front Immunol* 8, 1311, doi:10.3389/fimmu.2017.01311 (2017).
- 732 40 Pallett, L. J., Schmidt, N. & Schurich, A. T cell metabolism in chronic viral infection.
733 *Clin Exp Immunol* 197, 143-152, doi:10.1111/cei.13308 (2019).
- 734 41 Swamy, M. et al. Glucose and glutamine fuel protein O-GlcNAcylation to control T cell
735 self-renewal and malignancy. *Nat Immunol* 17, 712-720, doi:10.1038/ni.3439 (2016).
- 736 42 Liew, C. C., Ma, J., Tang, H. C., Zheng, R. & Dempsey, A. A. The peripheral blood
737 transcriptome dynamically reflects system wide biology: a potential diagnostic tool. *J*
738 *Lab Clin Med* 147, 126-132, doi:10.1016/j.lab.2005.10.005 (2006).
- 739 43 Xiong, Y. et al. Transcriptomic characteristics of bronchoalveolar lavage fluid and
740 peripheral blood mononuclear cells in COVID-19 patients. *Emerg Microbes Infect* 9,
741 761-770, doi:10.1080/22221751.2020.1747363 (2020).
- 742 44 Wong, K. L. et al. The three human monocyte subsets: implications for health and
743 disease. *Immunol Res* 53, 41-57, doi:10.1007/s12026-012-8297-3 (2012).
- 744 45 Liu, J. et al. Longitudinal characteristics of lymphocyte responses and cytokine profiles
745 in the peripheral blood of SARS-CoV-2 infected patients. *EBioMedicine* 55, 102763,
746 doi:10.1016/j.ebiom.2020.102763 (2020).
- 747 46 Wang, F. et al. Characteristics of peripheral lymphocyte subset alteration in COVID-
748 19 pneumonia. *J Infect Dis*, doi:10.1093/infdis/jiaa150 (2020).
- 749 47 Wen, W. et al. Immune cell profiling of COVID-19 patients in the recovery stage by
750 single-cell sequencing. *Cell Discov* 6, 31, doi:10.1038/s41421-020-0168-9 (2020).
- 751 48 Zhang, D. et al. COVID-19 infection induces readily detectable morphological and
752 inflammation-related phenotypic changes in peripheral blood monocytes, the severity
753 of which correlate with patient outcome. medRxiv preprint doi:
754 <https://doi.org/10.1101/2020.03.24.20042655>. , doi:10.1101/2020.03.24.20042655
755 (2020).
- 756 49 Zhou, R. et al. Acute SARS-CoV-2 Infection Impairs Dendritic Cell and T Cell
757 Responses. *Immunity*, doi:10.1016/j.immuni.2020.07.026 (2020).
- 758 50 Silvin, A. et al. Elevated Calprotectin and Abnormal Myeloid Cell Subsets Discriminate
759 Severe from Mild COVID-19. *Cell*, doi:10.1016/j.cell.2020.08.002 (2020).
- 760 51 Takahashi, T. et al. Sex differences in immune responses that underlie COVID-19
761 disease outcomes. *Nature*, doi:10.1038/s41586-020-2700-3 (2020).
- 762 52 Schulte-Schrepping, J. et al. Severe COVID-19 Is Marked by a Dysregulated Myeloid
763 Cell Compartment. *Cell*, doi:10.1016/j.cell.2020.08.001 (2020).
- 764 53 Jiang, Y. et al. COVID-19 pneumonia: CD8(+) T and NK cells are decreased in number
765 but compensatory increased in cytotoxic potential. *Clin Immunol* 218, 108516,
766 doi:10.1016/j.clim.2020.108516 (2020).
- 767 54 Christopher Maucourant, I. F., Andrea Ponzetta, Soo Aleman, Martin Cornillet, Laura
768 Hertwig Benedikt Strunz, Antonio Lentini, Björn Reinius, Demi Brownlie, Angelica
769 Cuapio Gomez, Eivind Heggernes Ask, Ryan M. Hull, Alvaro Haroun-Izquierdo, Marie
770 Schaffer, Jonas Klingström, Elin Folkesson, Marcus Buggert, Johan K. Sandberg, Lars
771 I. Eriksson, Olav Rooyackers, Hans-Gustaf Ljunggren, Karl-Johan Malmberg, Jakob
772 Michaëlsson, Nicole Marquardt, Quirin Hammer, Kristoffer Strålin, Niklas K.
773 Björkström; and the Karolinska COVID-19 Study Group. Natural killer cell
774 immunotypes related to COVID-19 disease severity. *Science Immunology*,
775 doi:10.1126/sciimmunol.abd6832 (2020). (2020).
- 776 55 Diao, B. et al. Reduction and Functional Exhaustion of T Cells in Patients With
777 Coronavirus Disease 2019 (COVID-19). *Front Immunol* 11, 827,
778 doi:10.3389/fimmu.2020.00827 (2020).

- 779 56 Katsuyama, E. et al. The CD38/NAD/SIRTUIN1/EZH2 Axis Mitigates Cytotoxic CD8 T
780 Cell Function and Identifies Patients with SLE Prone to Infections. *Cell Rep* 30, 112-
781 123 e114, doi:10.1016/j.celrep.2019.12.014 (2020).
- 782 57 Zheng, H. Y. et al. Elevated exhaustion levels and reduced functional diversity of T
783 cells in peripheral blood may predict severe progression in COVID-19 patients. *Cell*
784 *Mol Immunol*, doi:10.1038/s41423-020-0401-3 (2020).
- 785 58 De Biasi, S. et al. Marked T cell activation, senescence, exhaustion and skewing
786 towards TH17 in patients with COVID-19 pneumonia. *Nat Commun* 11, 3434,
787 doi:10.1038/s41467-020-17292-4 (2020).
- 788 59 Zeng, Y. et al. Peripheral Blood Mononuclear Cell Metabolism Acutely Adapted to
789 Postprandial Transition and Mainly Reflected Metabolic Adipose Tissue Adaptations
790 to a High-Fat Diet in Minipigs. *Nutrients* 10, doi:10.3390/nu10111816 (2018).
- 791 60 Codo, A. C. et al. Elevated Glucose Levels Favor SARS-CoV-2 Infection and Monocyte
792 Response through a HIF-1alpha/Glycolysis-Dependent Axis. *Cell Metab*,
793 doi:10.1016/j.cmet.2020.07.007 (2020).
- 794 61 Jaiswal, N., Agrawal, S. & Agrawal, A. High fructose-induced metabolic changes
795 enhance inflammation in human dendritic cells. *Clin Exp Immunol* 197, 237-249,
796 doi:10.1111/cei.13299 (2019).
- 797 62 Di Wu, T. S., Xiaobo Yang, Jian-Xin Song Mingliang Zhang Chengye Yao Wen Liu,
798 Muhan Huang, Yuan Yu, Qingyu Yang Tingju Zhu, Jiqian Xu, Jingfang Mu, Yaxin
799 Wang, Hong Wang, Tang Tang, Yujie Ren Yongran Wu, Shu-Hai Lin, Yang Qiu, Ding-
800 Yu Zhang, You Shang, Xi Zhou. Plasma Metabolomic and Lipidomic Alterations
801 Associated with COVID-19. *Natl Sci Rev*, doi:10.1093/nsr/nwaa086 (2020).
- 802 63 Max W. S. Oliveira, J. B. M., Marcos R. de Oliveira, Alfeu Zanotto-Filho, Guilherme A.
803 Behr, Ricardo F. Rocha, José C. F. Moreira, Fábio Klamt. Scavenging and antioxidant
804 potential of physiological taurine concentrations against different reactive
805 oxygen/nitrogen species. *Pharmaceutical Reports* 62, 185-193 (2010).
- 806 64 Cunningham, L., Simmonds, P., Kimber, I., Basketter, D. A. & McFadden, J. P. Perforin
807 and resistance to SARS coronavirus 2. *J Allergy Clin Immunol* 146, 52-53,
808 doi:10.1016/j.jaci.2020.05.007 (2020).
- 809 65 Maskus, D. J. et al. Characterization of a novel inhibitory human monoclonal antibody
810 directed against Plasmodium falciparum Apical Membrane Antigen 1. *Sci Rep* 6,
811 39462, doi:10.1038/srep39462 (2016).
- 812 66 Lorenz, M. A., Burant, C. F. & Kennedy, R. T. Reducing time and increasing sensitivity
813 in sample preparation for adherent mammalian cell metabolomics. *Anal Chem* 83,
814 3406-3414, doi:10.1021/ac103313x (2011).
- 815 67 Marimuthu, R. et al. Characterization of Human Monocyte Subsets by Whole Blood
816 Flow Cytometry Analysis. *J Vis Exp*, doi:10.3791/57941 (2018).
- 817 68 Autissier, P., Soulas, C., Burdo, T. H. & Williams, K. C. Evaluation of a 12-color flow
818 cytometry panel to study lymphocyte, monocyte, and dendritic cell subsets in humans.
819 *Cytometry A* 77, 410-419, doi:10.1002/cyto.a.20859 (2010).
- 820 69 Davies, R., Vogelsang, P., Jonsson, R. & Appel, S. An optimized multiplex flow
821 cytometry protocol for the analysis of intracellular signaling in peripheral blood
822 mononuclear cells. *J Immunol Methods* 436, 58-63, doi:10.1016/j.jim.2016.06.007
823 (2016).
- 824



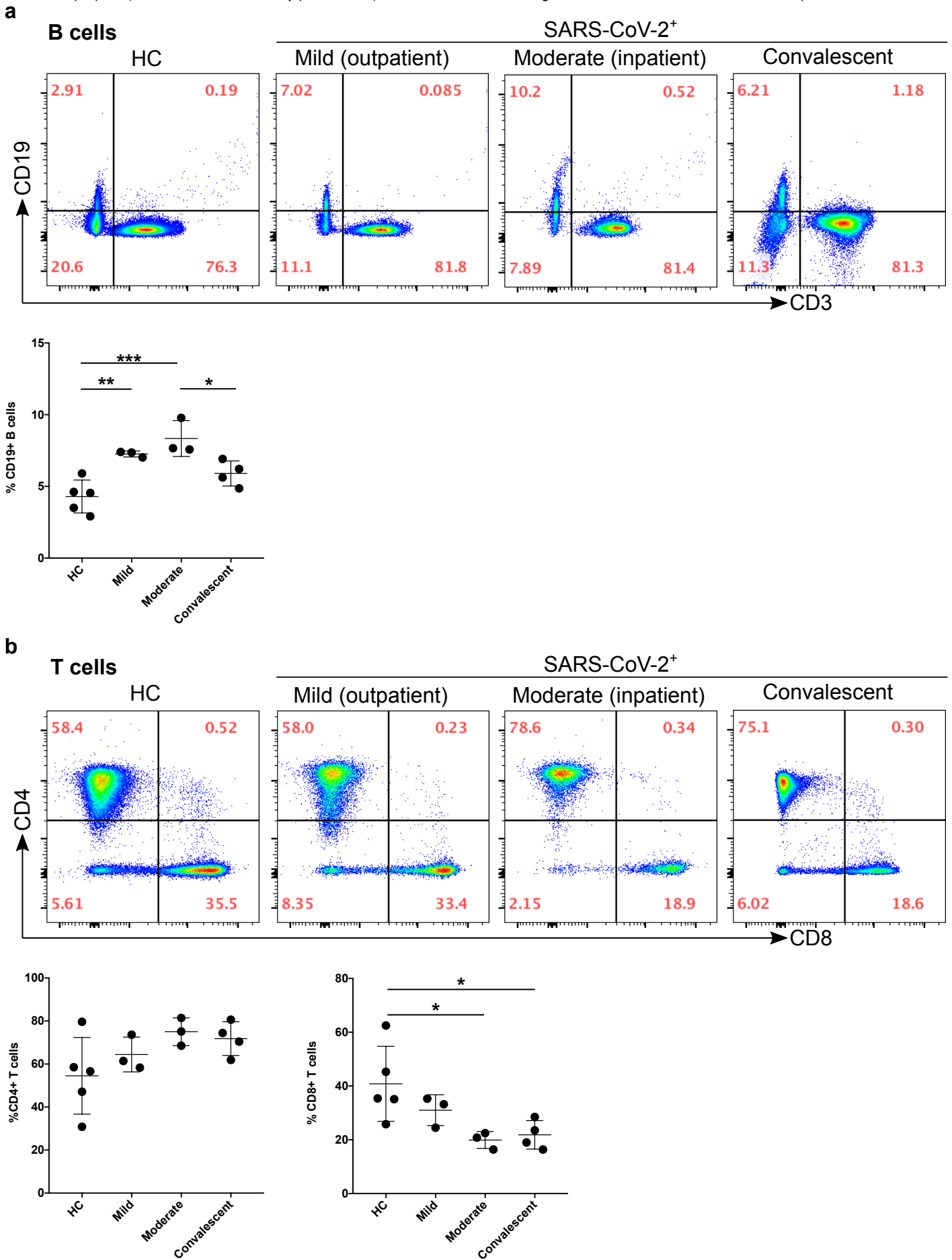


Fig. 2

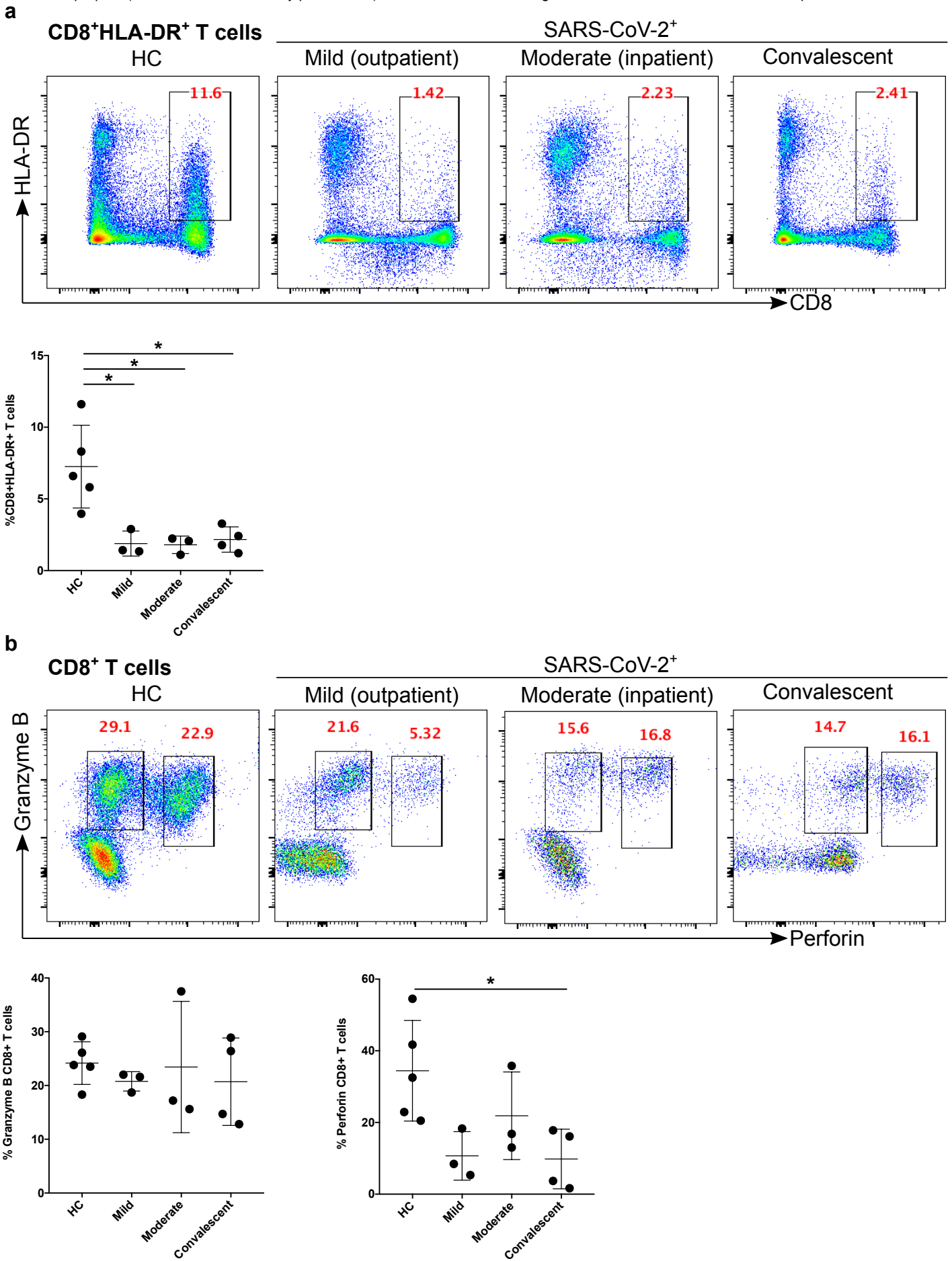
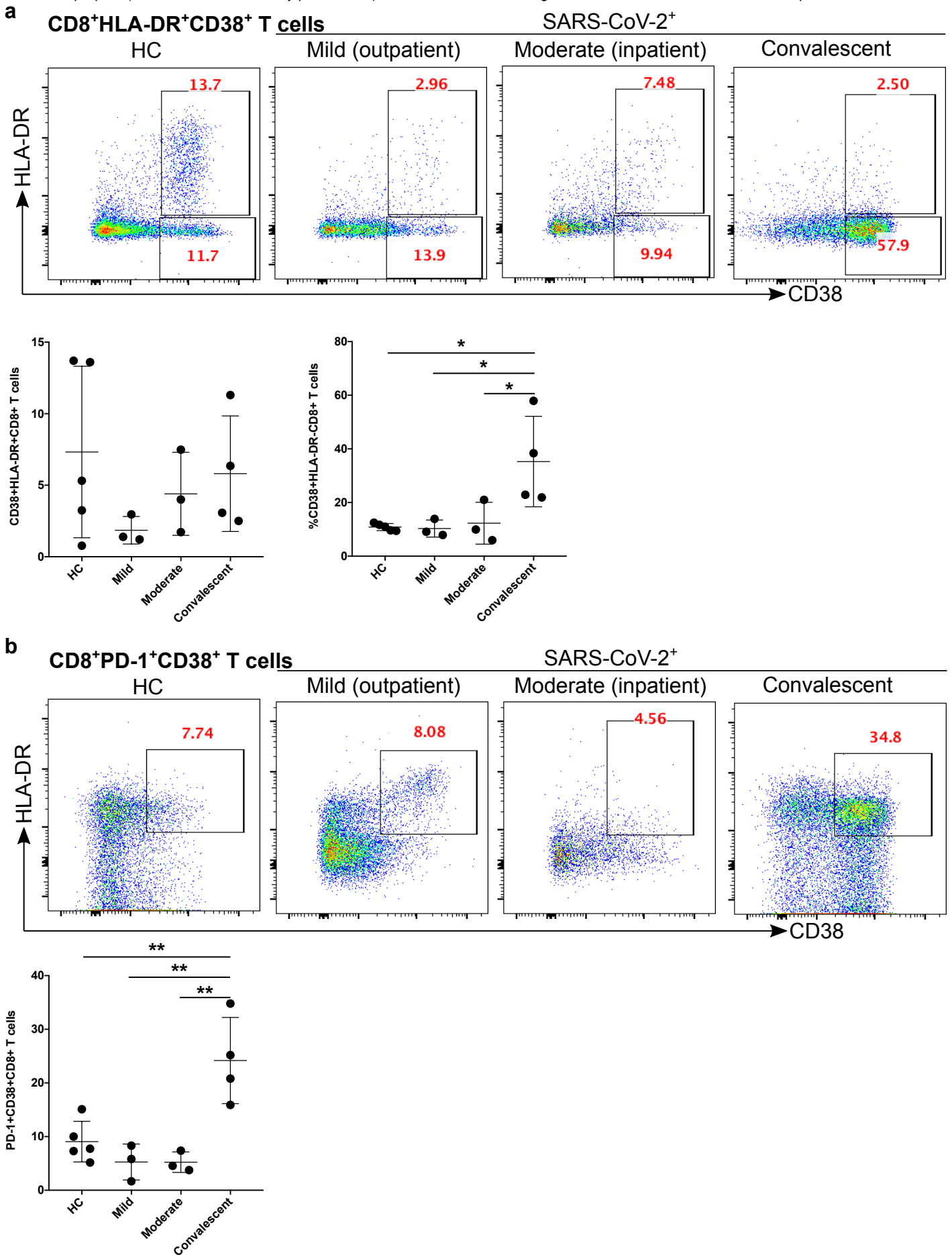


Fig. 3



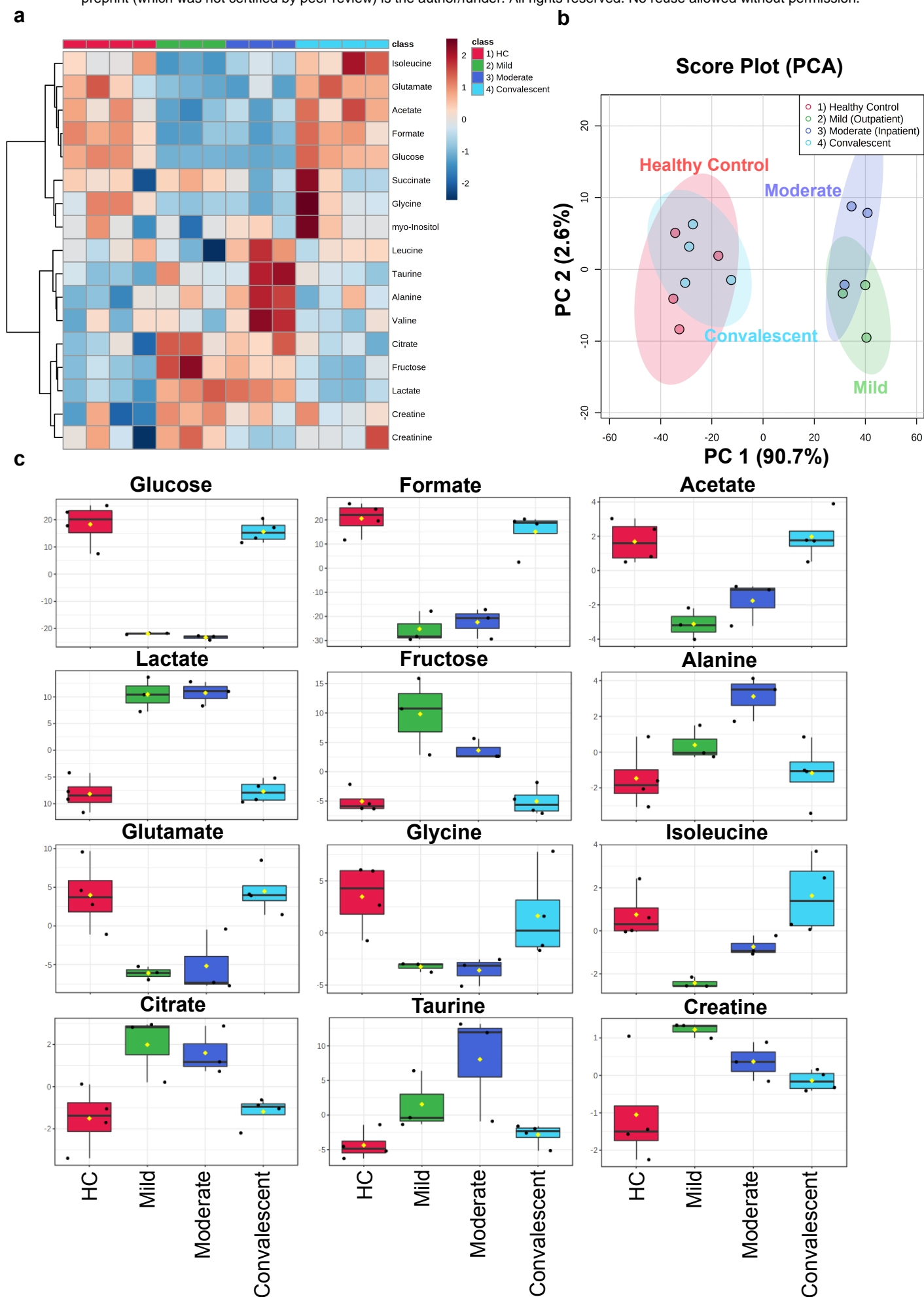
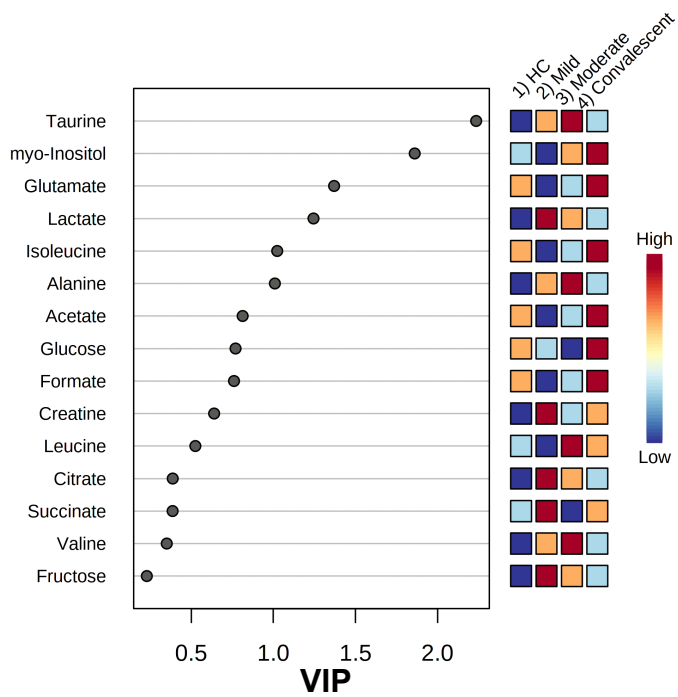
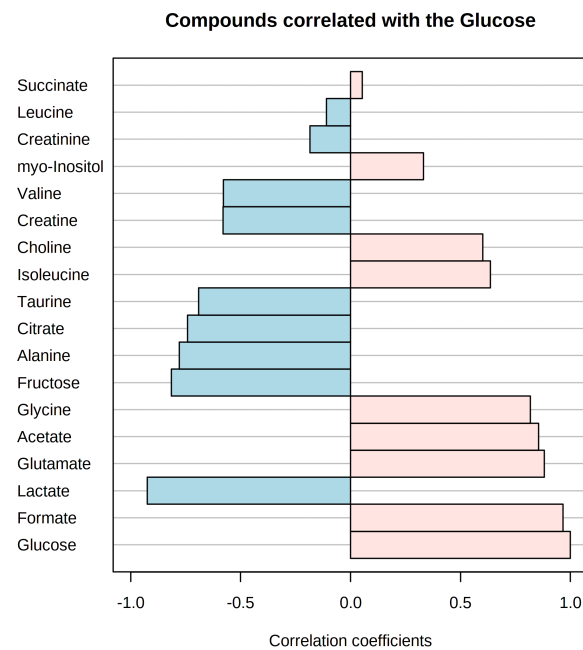


Fig. 5

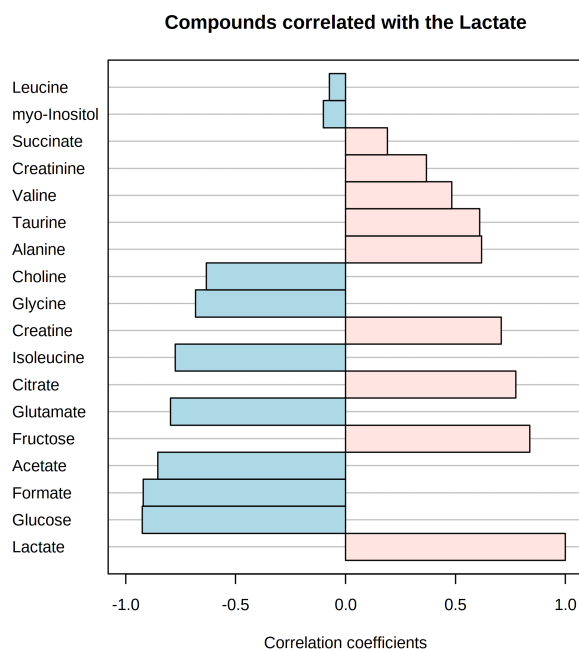
a



b



c



Compounds correlated with the Fructose

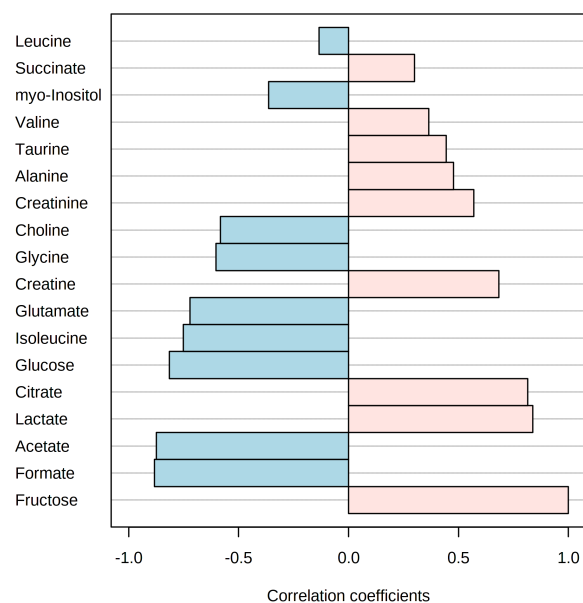
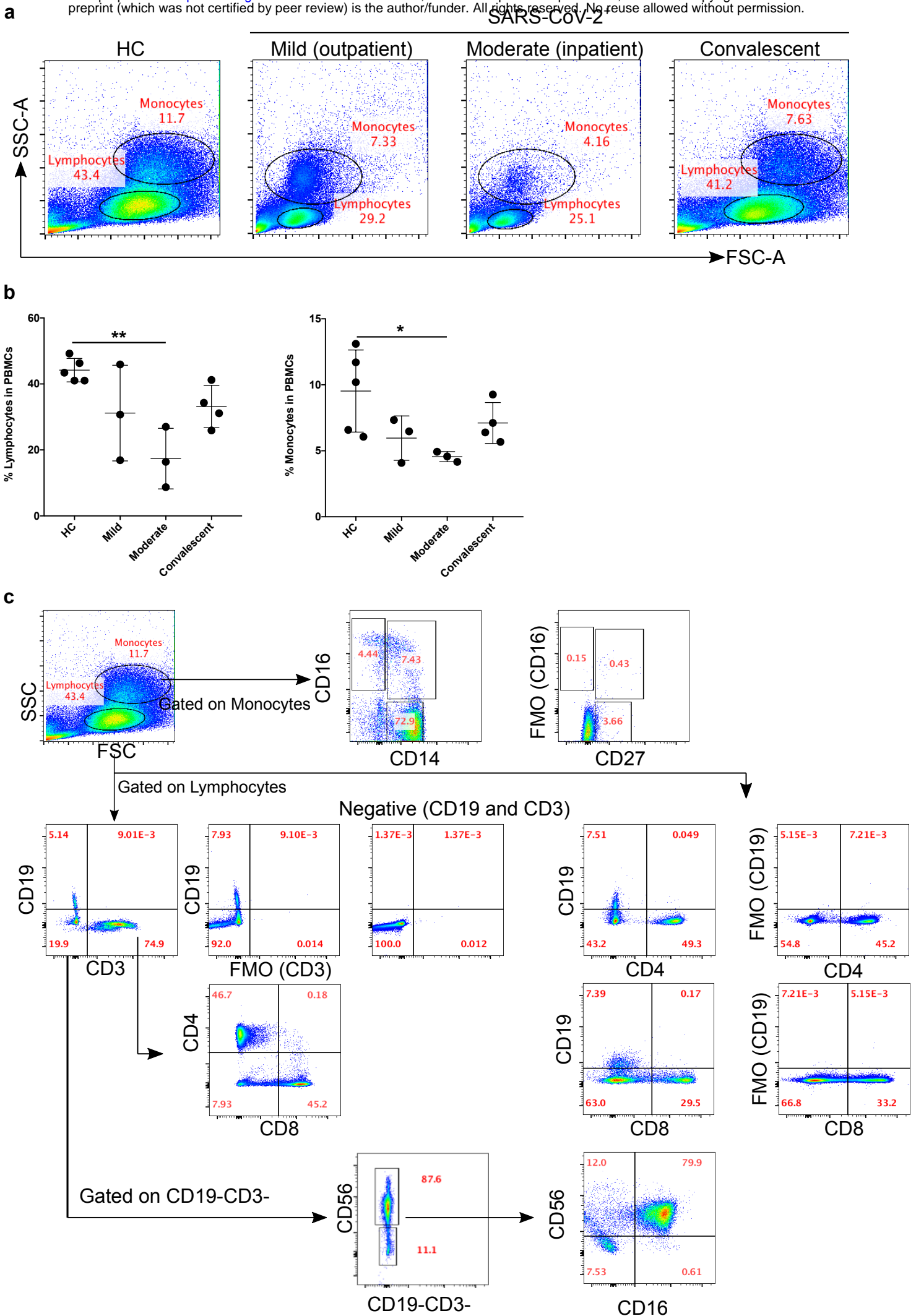
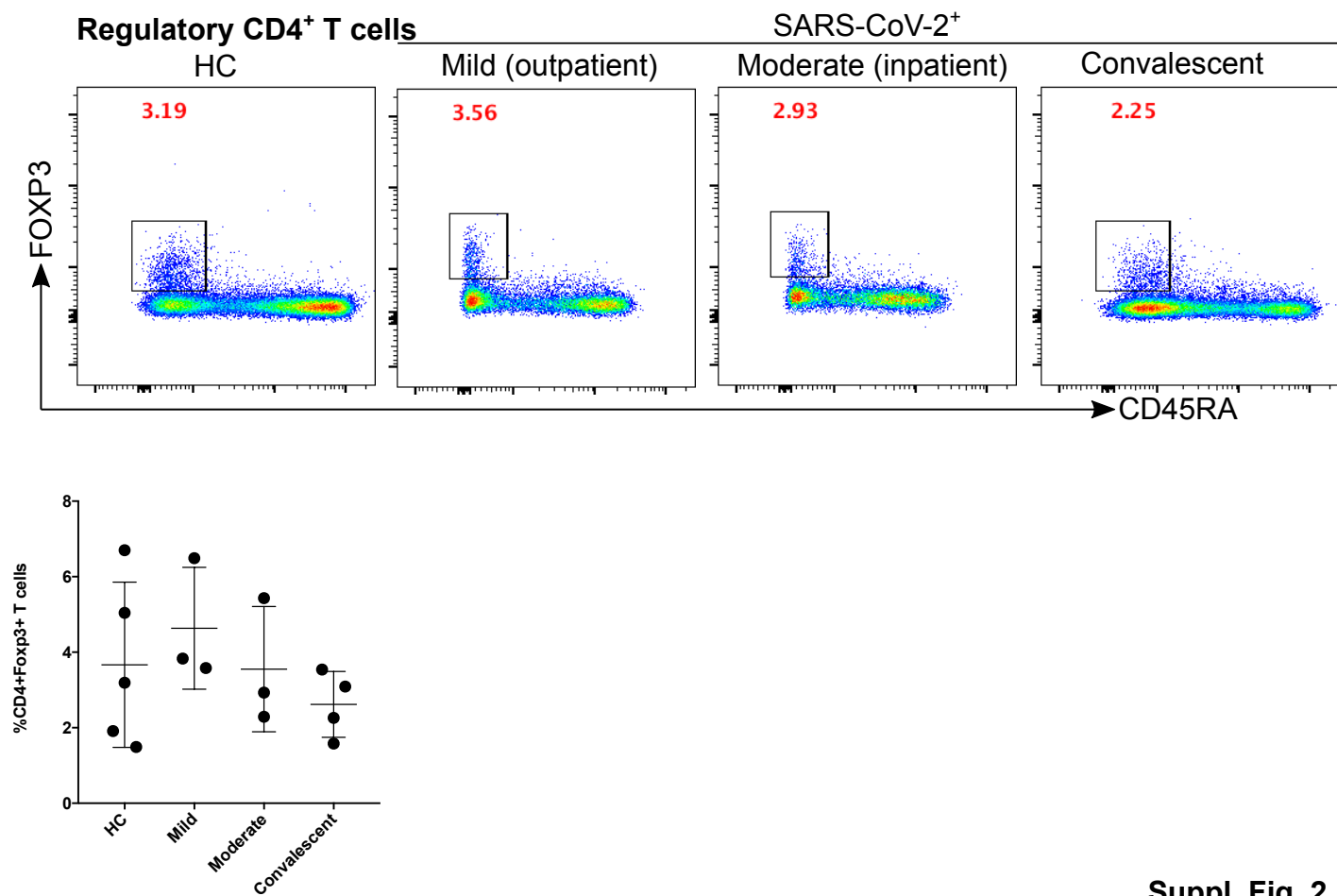


Fig. 6

SARS-CoV-2





Suppl. Fig. 2

